ARTICLE OPEN

Check for updates

Translational reprogramming of dentate gyrus peptidergic circuitry gates antidepressant efficacy

Seo-Jin Oh[1,2,8], Jin-hyeok Jang[1,2,8], Jean-Pierre Roussarie[3], Gyeong-un Jang[1], Min-seok Jeong[1], Yeon Suk Jo[1], Chang-Hoon Shin[1,4], Hongsoo Choi[5], Kwang Lee[1], Jong Hyuk Yoon[6] and Yong-Seok Oh[1,7]✉

Selective serotonin reuptake inhibitors (SSRIs) exhibit delayed therapeutic effects despite rapid serotonin elevation, suggesting their dependence on slow neuroplastic adaptations. Here, we demonstrate that antidepressant actions require cell type-specific translational regulation of the peptidergic signaling in the dentate gyrus (DG). Chronic, but not acute, treatment with an SSRI fluoxetine (FLX) selectively enhances translational activity in hilar mossy cells (MCs), with no detectable changes in neighboring granule cells (GCs). Combining Translating Ribosome Affinity Purification (TRAP) with RNA sequencing revealed distinct baseline translatomes between these two glutamatergic neurons and identified FLX-induced remodeling of peptidergic pathways in the DG. Crucially, we discovered MC-specific enrichment of the neuropeptide PACAP, which undergoes translation-dependent upregulation by chronic FLX treatment. This PACAP induction mediates neuroadaptive plasticity in PAC1 receptor-expressing GCs and drives behavioral responses prominently in female mice during prolonged FLX administration. Our findings establish cell type-specific translational reprogramming as a novel mechanistic framework for antidepressant action.

Molecular Psychiatry; https://doi.org/10.1038/s41380-026-03461-2

INTRODUCTION

Major depressive disorder (MDD) is a highly prevalent psychiatric condition characterized by chronicity, recurrence, and potential life-threatening consequences [1]. Selective serotonin reuptake inhibitors (SSRIs) are the most widely prescribed medications for MDD treatment. While SSRIs quickly increase extracellular serotonin levels within hours, the therapeutic effects take longer as neural circuitry needs to adapt to these neurochemical changes over several weeks [2, 3]. This therapeutic delay is likely due to the gradual, neuroplastic adaptations in the neural circuit, in response to sustained serotonin levels [4, 5]. Recent hypotheses have proposed that long-term alterations in neural circuitry, involving changes in gene transcription and protein translation within specific neuronal subtypes, contribute to the pathogenesis of MDD and its response to antidepressant medication [6–8]. Nevertheless, our current knowledge regarding the precise therapeutic mechanisms of SSRIs at the level of distinct neuronal cell types and key molecules remains incomplete.

The mRNA translational control is associated with the onset of psychiatric disorders and their therapeutic recovery [9–12]. The mTOR signaling pathway, a pivotal regulator of translational control, plays a crucial role in both the pathophysiology of MDD and the pharmacological effects of antidepressants [10, 12–14]. Notably, genetic inhibition of eukaryotic translation initiation factor 4E (eIF4E) or ribosomal protein S6 Kinase 1 signaling (S6K1), a key component in the mTOR signaling pathway, not only induces depressive-like behaviors but also abolishes the antidepressant effects of both SSRIs and ketamine [10, 12, 14]. Similarly, pharmacological intervention of mTOR signaling with rapamycin cancels antidepressant effects [15, 16]. While most studies of antidepressant action have concentrated on transcriptional mechanisms [17–19], translational analysis provides a more functionally relevant perspective. Unlike transcriptional profiling, which measures the total pool of mRNAs, translational approaches capture the subset of transcripts actively engaged in de novo protein synthesis [20], thereby better reflecting changes that ultimately shape protein expression and cellular function. Despite the growing evidence for pivotal role of translational control for antidepressant actions, it remains largely unknown whether this process occurs in a cell type-specific manner and which genes are regulatory targets within the affected cell types.

The hippocampus is known to be extensively implicated in the pathophysiology of MDD and the pharmacological action of antidepressants [21, 22]. Specifically, among the subregions of the hippocampus, the dentate gyrus (DG), which receives prominent monoaminergic inputs, has been implicated in response to various antidepressant drugs [23–26]. The DG represents a key brain region where neuroplasticity including neurogenesis is induced by psychotropic medications [21, 26–30]. Within the DG, the major neuronal subtypes, granule cells (GCs) and mossy cells (MCs), play integral and interdependent roles in hippocampal functions [31, 32]. Chronic antidepressant treatment induces substantial

[1]Department of Brain Science, DGIST, Hyeonpung-eup, Dalseong-gun, Daegu, Republic of Korea. [2]Convergence Research Advanced center for Olfaction, DGIST, Hyeonpung-eup, Dalseong-gun, Daegu, Republic of Korea. [3]Department of Anatomy and Neurobiology, Boston University Chobanian & Avedisian School of Medicine, Boston, MA, USA. [4]Preclinical Research Center, Daegu-Gyeongbuk Medical Innovation Foundation, Daegu, Republic of Korea. [5]Department of Robotics Engineering, DGIST, Hyeonpung-eup, Dalseong-gun, Daegu, Republic of Korea. [6]Neurodegenerative Disease Research Group, Korea Brain Research Institute, Daegu, Republic of Korea. [7]Brain Engineering Convergence Research Center, DGIST, Hyeonpung-eup, Dalseong-gun, Daegu, Republic of Korea. [8]These authors contributed equally: Seo-Jin Oh, Jin-hyeok Jang. ✉email: ysoh2040@dgist.ac.kr

Received: 30 May 2025 Revised: 22 December 2025 Accepted: 25 January 2026
Published online: 03 February 2026

alteration in gene transcription and neuronal activity in GCs and MCs, which are crucial for SSRI actions in the hippocampus [8, 24, 26, 29, 33, 34]. However, research on the translational regulation of these two neuronal populations by the antidepressant and its impact on the drug actions remains unexplored.

In this study, we observed that chronic treatment of an SSRI FLX induces differential effects on translational activity of DG neuronal cell types. Using the Translating Ribosome Affinity Purification (TRAP) approach, we isolated and profiled the translatome of MCs and GCs to perform a genome-wide assessment of active mRNA translation. Our analysis revealed cell type-specific translatome profiles and, crucially, identified translational reprogramming of key neuropeptidergic pathways in response to chronic FLX treatment. We found that the neuropeptide PACAP, encoded by the gene *Adcyap1* is translationally upregulated specifically in MCs. This PACAP induction mediates the neuroplasticity of PAC1 receptor-expressing GCs and drives behavioral recovery with a pronounced effect in female mice. Our findings establish a novel mechanistic framework antidepressant actions, centered on cell type-specific translational control of peptidergic circuits.

MATERIALS AND METHODS

Animals

All experimental procedures were approved by the Animal Care and Use Committee of the Daegu Gyeongbuk Institute of Science & Technology (IACUC #20011503-03) and of the Rockefeller University (IACUC #14686-H). Transgenic mouse lines were used in this study : The Eef1a-LSL-EGFPL10 TG (JAX stock, #030305), Drd2-Cre TG (GENSAT, Clone #ER44), MC-TRAP (Drd2-Cre;Eef1a1$^{LSL.EGFPL10a/+}$), Sstr4-bacTRAP mice. The mouse breeding methods and housing conditions are described in Supplementary Materials and Methods.

Drug treatments

Details of drug treatments were included in Supplementary Materials and Methods.

Immunohistochemistry

All mice were perfused transcardially with PBS, followed by 4% paraformaldehyde (PFA) in PBS and post-fixed in the same solution overnight at 4 °C. The brains were coronally or horizontally cut into 40-µm-thick sections with a Cryostat (CM3050S, Leica). Sections were processed using a free-floating procedure. Detailed description of antibody preparation, antigen retrieval, image acquisition, and quantification are provided in Supplementary Materials and Methods.

Image analysis

Fluorescence images were acquired using a Zeiss LSM 800 confocal microscope (Carl Zeiss, Germany) equipped with a 10x and 20x objective. Maximum intensity projections were generated in Zen Blue software (Carl Zeiss, Germany). For quantification of fluorescence intensity, images were processed using ImageJ (FIJI, NIH, USA). See detailed methods in Supplementary Materials and Methods.

TRAP assay

TRAP assay was conducted with minor modifications of the original procedure [35]. DG (MC & GC)-TRAP mice were used for DG translatome analysis. The TRAP assay is a technically demanding procedure; maintaining RNA integrity during immunoaffinity purification from tissue homogenates in an H_2O-based buffer is critical and limits the number of samples that can be processed simultaneously (a maximum of 12–14 per experiment). Detailed methods for tissue homogenization, polysome immunoprecipitation, and RNA purification are described in Supplementary Materials and Methods.

RNA-seq & data analysis

This analysis was described in detail in Supplementary Materials and Methods. The sequencing data for this study have been submitted to the NCBI Gene Expression Omnibus (GEO) under accession number GSE309750.

Quantitative real-type polymerase chain reaction (qPCR)

Details of qPCR methods and primers information were included in Supplementary Materials and Methods.

Western blots

After treatment of antidepressant drug (15 mg kg^{-1}day^{-1}) or saline for 2 weeks, the mice were sacrificed, and the brains were extracted. The detailed methods are described in Supplementary Materials and Methods.

Stereotaxic surgery

Stereotaxic injection of AAV was carried out on a stereotaxic frame for mice (Angle Two^{TM}, Leica, USA). Mice were anesthetized by intraperitoneal injection of Avertin (250 mg/kg), and viral constructs (AAV2-U6-ShRNA-mADCYAP1-CMV-EGFP-SV40, AAV2-U6-ShRLuc-CMV-EGFP-SV40) were stereotaxically injected bilaterally into the dentate hilus region (coordinates for Ventral : AP −3.3, ML ± 2.7, DV -3.6). See detailed methods in Supplementary Materials and Methods.

Restraint stress

Animals were subjected to restraint stress (2 hours/day) for 2 weeks, during which mice were individually placed in a restrainer tube (Jeungdo B&P, Korea). The tube has air holes for ventilation and limits for the mice's movement.

Behavior assessments

Depression and anxiety-related behaviors (novelty suppressed feeding [NSF] test, tail suspension test [TST], elevated plus maze [EPM], and light/dark box [LDB] test) and locomotor activity (open field [OF] test) were tested as described in Supplementary Materials and Methods.

BrdU labeling and neurogenesis assay

The mice were administered BrdU solution (200 mg/kg) intraperitoneally 3 h prior to sacrifice. To assess the differentiation of new neurons, a separate cohort of mice was processed for Doublecortin (DCX) immunohistochemistry. See detailed methods in Supplementary Materials and Methods.

In-situ hybridization assay

For detecting mRNA levels in situ, we performed using RNA scope™ chromogenic assay (Advanced Cell Diagnostics, Cat #322360) according to the manufacturer's protocol. See detailed methods in Supplementary Materials and Methods.

Statistics

Statistical analysis was conducted using GraphPad Prism Version 7.0a. Data was analyzed by a two-tailed *t*-test, one-way ANOVA, two-way ANOVA followed by the post hoc Tukey's test. All data are presented as means ± SEM. Significance thresholds were as follows: *$p < 0.05$, **$p < 0.01$, ***$p < 0.001$, ****$p < 0.0001$.

RESULTS

Effects of chronic FLX treatment on cell type-specific translational activation in the DG

Chronic antidepressant treatment induces neuroplastic changes through cell type-specific gene regulation in the neural circuitry, which may underlie the gradual onset of the antidepressive effects [7, 8, 36]. Here, we examined whether chronic antidepressant administration influences the translational activity of the DG neuronal subtypes in the restraint stress-induced depression model [37]. The animals, with or without chronic restraint stress, were treated either by vehicle (VEH) or an SSRI, fluoxetine (FLX; 15 mg/kg/day), daily for a period of 2 weeks (Fig. 1a). The FLX effect on translational activity was assessed by measuring the phosphorylation level of ribosomal S6 protein (rS6) in the hippocampal sections across the dorsoventral axis. Upon activation of the mTOR pathway, rS6 is phosphorylated at multiple sites, including serine residues 235/236 and 240/244 [38], which is considered a proxy marker for translational activation in given

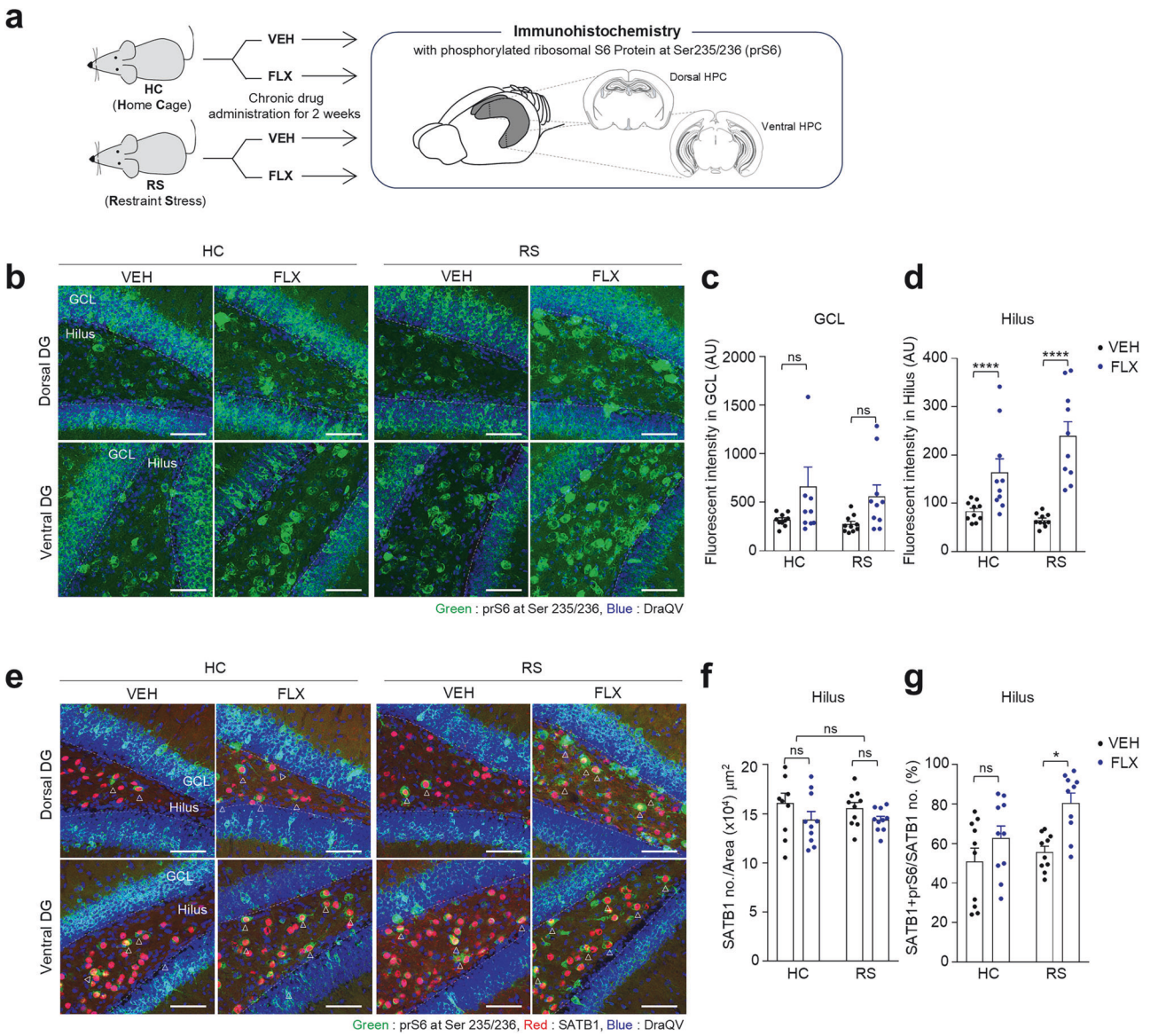

Fig. 1 Cell type-specific translational activation in the DG by chronic FLX treatment. a Schematic of the experimental paradigm. HC (Home Cage) and RS (Restraint Stress) mice administrated VEH (vehicle) or FLX (fluoxetine) for 2 weeks (all male mice; HC:VEH, $n = 10$; HC:FLX, $n = 10$; RS:VEH, $n = 10$; RS:FLX, $n = 10$). Hippocampal sections across the dorsoventral axis were subjected to immunostaining with phosphorylated ribosomal S6 protein specific antibodies. **b** Representative images with prS6 at Ser 235/236 immuno-staining results. Scale bar; 100 μm. **c** Quantification of fluorescent intensity of prS6 signals in the GCL. Two-way ANOVA, [Stress x drug interaction $F(1, 36) = 0.062$; $p = 0.8041$; main effect of stress: $F(1, 36) = 0.3924$; $p = 0.535$; main effect of fluoxetine: $F(1, 36) = 7.322$; $p = 0.0103$], followed by the Tukey's post hoc test. Tukey's multiple comparisons test [HC:VEH vs. HC:FLX; $p = 0.1757$, RS:VEH vs. RS:FLX; $p = 0.3202$]. **d** Quantification of fluorescent intensity of prS6 signals in the hippocampal hilus. Two-way ANOVA, [Stress x drug interaction $F(1, 36) = 5.083$; $p = 0.0303$; main effect of stress: $F(1, 36) = 1.865$; $p = 0.1805$; main effect of fluoxetine: $F(1, 36) = 38.03$; $p < 0.0001$], followed by the Tukey's post hoc test. Tukey's multiple comparisons test [HC:VEH vs. HC:FLX; $p = 0.0422$, RS:VEH vs. RS:FLX; $p < 0.0001$]. **e** Representative double-immunolabeling images of prS6-positive cells (Green) with MC marker SATB1 (Red). The empty arrowhead indicates colocalization of prS6 and SATB1. Scale bar; 100 μm. **f** Quantification of SATB1-positive cell number relative to hilus area. Two-way ANOVA, [Stress x drug interaction $F(1, 36) = 0.1159$; $p = 0.7355$; main effect of stress: $F(1, 36) = 0.125$; $p = 0.7247$; main effect of fluoxetine: $F(1, 36) = 3.789$; $p = 0.0594$], followed by the Tukey's post hoc test. Tukey's multiple comparisons test [HC:VEH vs. HC:FLX; $p = 0.3821$, RS:VEH vs. RS:FLX; $p = 0.6702$]. **g** Quantification of SATB1 and prS6-double positive cell number relative to total SATB1-positive cell number. Two-way ANOVA, [Stress x drug interaction $F(1, 36) = 1.472$; $p = 0.2329$; main effect of stress: $F(1, 36) = 4.433$; $p = 0.0423$; main effect of fluoxetine: $F(1, 36) = 11.67$; $p = 0.0016$], followed by the Tukey's post hoc test. Tukey's multiple comparisons test [HC:VEH vs. HC:FLX; $p = 0.415$, RS:VEH vs. RS:FLX; $p = 0.012$]. Data are represented as means ± SEM. Pair-wise comparison by post hoc test; *$p < 0.05$, ****$p < 0.0001$, ns, non-significant. HC, home cage; RS, restraint stress; DG, dentate gyrus; GCL, granule cell layer; VEH, vehicle; FLX, fluoxetine. See also Figure S1, and S2.

cells [39–41]. Chronic SSRI administration increases the rS6 phosphorylation (prS6) at Ser 235/236 and 240/244 in the DG, which is prominent in the hilus, but not in the granule cell layer (GCL) (Fig. 1b – d, S1a–S1c). To ascertain the identity of the hilar cell type in which rS6 is phosphorylated in response to the drug, we performed double immuno-staining with the MCs marker SATB1 [42] (Fig. 1e). While the number of SATB1-positive MCs remains consistent among all comparison groups (Fig. 1f), the number of prS6- and SATB1-double positive MCs exhibits a notable increase only in the group with chronic FLX

administration (Fig. 1g), suggesting FLX regulation of translational activity in MCs. However, this observation is not replicated with acute FLX administration, even with marginal increase of SATB1 immunoreactivity, indicating that the duration of drug administration is crucial for translational activation in MCs (Fig. S2a–S2J). In essence, chronic FLX treatment differentially influences the translational activity of each neuronal subtype in the DG, with a notable augmentation in MCs, thereby highlighting them as a critical node in the DG circuitry engaged by chronic antidepressant treatment.

Distinct translatomic profiles of MCs and GCs

To profile the translational features of two principal neuronal subtypes, GCs and MCs, within the DG, we employed the TRAP analysis, which utilizes the cell type-specific expression of an EGFP-tagged ribosomal L10a subunit (EGFP-L10a) and its biochemical fractionation of actively translating mRNA with EGFP affinity purification (Fig. 2a). In MC-TRAP mice, EGFP-L10a expression is observed in the hilus across the dorsoventral axis of the DG and also much less in the CA subfields. The EGFP-L10a colocalizes with GluR2/3 and Calb2, an MC marker (Fig. S3a). In the ventral hilus, approximately 95% of MCs colocalize with Calb2, a well-established marker for ventral MCs (Fig. S3a). Moreover, EGFP-labeled hilar neurons exhibit substantial colocalization with the MC marker GluR2/3 across the dorsoventral axis, further confirming their identity as MCs (Fig. S3a). Similarly, EGFP-L10a expression in GC-TRAP mice is detected specifically within the granule cell layer (Fig. S3b). This EGFP labeling exhibits complete colocalization with Prox1 in the dorsal and medial region, gradually weakening toward the ventral pole. This IHC analysis confirms the cell type-specific expression of EGFP-L10a in each transgenic mouse line. Next, we conducted a TRAP assay to isolate translatomes from each cell type and examined whether cell type-specific markers are enriched through TRAP assay. To achieve this, we performed qPCR analysis to assess the expression level of cell type-specific marker genes in the isolated translatomes (IP) compared to the hippocampal homogenate controls (HC). We found a more than 20-fold enrichment of *Calb2* and *Cyp26b1* in the MC translatome (Fig. S3c), which is consistent with previous reports [43, 44]. In parallel, we observed approximately 10-fold and 5-fold enrichment of GC markers *Prox1* and *Calb1*, respectively, in the GC translatome (Fig. S3d). These results collectively demonstrate that MC-TRAP and GC-TRAP mice are suitable for profiling cell type-specific translatomes in the DG.

Next, we profiled translatomic features of MCs and GCs in the DG. To this end, we conducted high-throughput RNA sequencing analysis to perform a genome-wide assessment of active ribosomal complex-bound mRNAs tagged in MC-TRAP and GC-TRAP mice (Fig. 2a). Initially, we compared the cell type-specific translatomes of MCs and GCs with the unbound hippocampal homogenate controls (HC). This analysis led to the identification of 952 enriched genes and 1542 depleted genes in MCs, as well as 625 enriched genes and 675 depleted genes in GCs (FDR < 0.05; Fig. 2b, Table S1). By organizing the enriched or depleted genes in MCs and GCs into a Venn diagram, we found that the two neuron types exhibit distinct translational profiles, with a subset of genes overlapping between them (Fig. 2c). Furthermore, we conducted a 9-quadrant association analysis of mRNA by plotting scatter plots of these genes, which allowed us to extract specific genes that are highly enriched in MCs and GCs (Fig. 2d). Notably, *Calb1* and *Drd1* are known to be highly enriched in GCs [24, 45], whereas *Calb2* and *Drd2* are highly enriched in MCs [46, 47]. We also identified cell type-specific markers including *Gal*, *Glp1r*, and *Rgs12* for MCs as well as *Plekha2*, *Pdzd2*, and *Parvg* for GCs, and further validated their expression using the in-situ hybridization (ISH) database from the Allen Brain Atlas (Fig. 2e, f).

In addition, both MCs and GCs are glutamatergic neurons that share developmental origins [48]. Nevertheless, as different neuronal populations, they are expected to exhibit cell type-specific molecular features at baseline. To capture such cell type-specific features in our dataset, we conducted a direct comparison of the TRAP data through volcano plot analysis. Our analysis reveals 1729 genes enriched in MCs relative to GCs and 2121 genes enriched in GCs, relative to MCs (Fig. 2g, Table S1). To gain insights into the characteristics of these gene sets, we performed enrichment analysis. Synaptic transmission, encompassing neurotransmitter and neuropeptide signaling, exhibits significant enrichment in the MC translatome (Fig. 2h). Conversely, transcription, cell differentiation, and metabolic pathways are prominently enriched in the GC translatome (Fig. 2i). We further examined the relative distribution of neurotransmitter receptors by comparing MCs or GCs to the entire hippocampus (HC) or through direct comparison between MCs and GCs (Fig. 2j). Neurotransmitter receptors exhibit distinct expression patterns depending on the cell types. Among them, ionotropic glutamatergic receptors such as *Grin2d*, *Grin3a*, and *Grik1* demonstrate differential expression across cell types, with notably higher levels in MCs. Similarly, metabotropic receptors, including *Grm4* and *Grm8*, are also enriched in MCs. Interestingly, serotonin receptors which are key mediators for antidepressant responses, *Htr2a* and *Htr4* are enriched in MCs and GCs, respectively. Dopamine receptors D1 (*Drd1*) is also enriched in the GCs, while *Drd2* is highly enriched in the MCs, which is consistent with previous findings [49]. In addition, other monoamine receptors including *Adra1b, Adra2a, Adra2c, Hrh2*, and *Hrh3*, exhibit cell type-specific expression patterns, with many of these receptors showing a tendency for enhanced expression in MCs. A wide range of neuromodulatory receptors for neuro-endocrine hormones, nucleotides, and bioactive lipid ligands also display distinct expression profiles between the two cell types, with a significant number being enriched in MCs. Together, these findings establish that MCs and GCs possess highly distinct baseline translatomes, with the MC translatome being uniquely specialized for synaptic and neuromodulatory signaling. This positions MCs as potential key integrators of diverse inputs to the DG circuit.

Regulation of cell type-specific translatome by chronic FLX treatment

Based on our finding of FLX-induced translational activation in the DG (Fig. 1), we next performed TRAP-seq to profile the specific translatomic changes in MCs and GCs in response to chronic FLX (15 mg/kg/day) for 2 weeks. This translatome profiling was conducted in stress-naïve animals for three key reasons: 1) our initial data showed that a key marker (prS6) was similarly upregulated in both stressed and naïve states (Fig. 1), allowing us to isolate the drug's core effects in a mechanistically clearer context; 2) This approach isolated the drug's specific molecular effects from the confounding background of stress; and 3) the technical throughput limitations of the TRAP assay precluded a more complex four-group factorial design (i.e., Naïve/Stressed × VEH/FLX). The antidepressant-like efficacy of this treatment regimen was confirmed using the tail-suspension and novelty-suppressed feeding tests (Fig. S4a, S4b).

Here, we profiled the FLX-responsive translatomes from MC-TRAP (VEH/FLX, n = 6/7) and GC-TRAP (VEH/FLX, n = 4/4). Next, differentially translated gene (DTG) analysis was performed (FDR < 0.05; Fig. 3a). Upon direct comparison between VEH and FLX conditions, a greater number of DTGs is observed in the cell type-specific translatomes compared to the differentially expressed genes (DEGs) in the hippocampal homogenate controls (HC). In the MC translatome, 930 genes are upregulated by chronic FLX treatment, while 79 genes are downregulated (Fig. 3b). In the GC translatome, 951 genes are upregulated, and 873 genes are downregulated (Fig. 3c). In contrast, a relatively smaller number of genes is found to be transcriptionally upregulated (192 genes) and downregulated (30 genes) in the total hippocampal homogenate

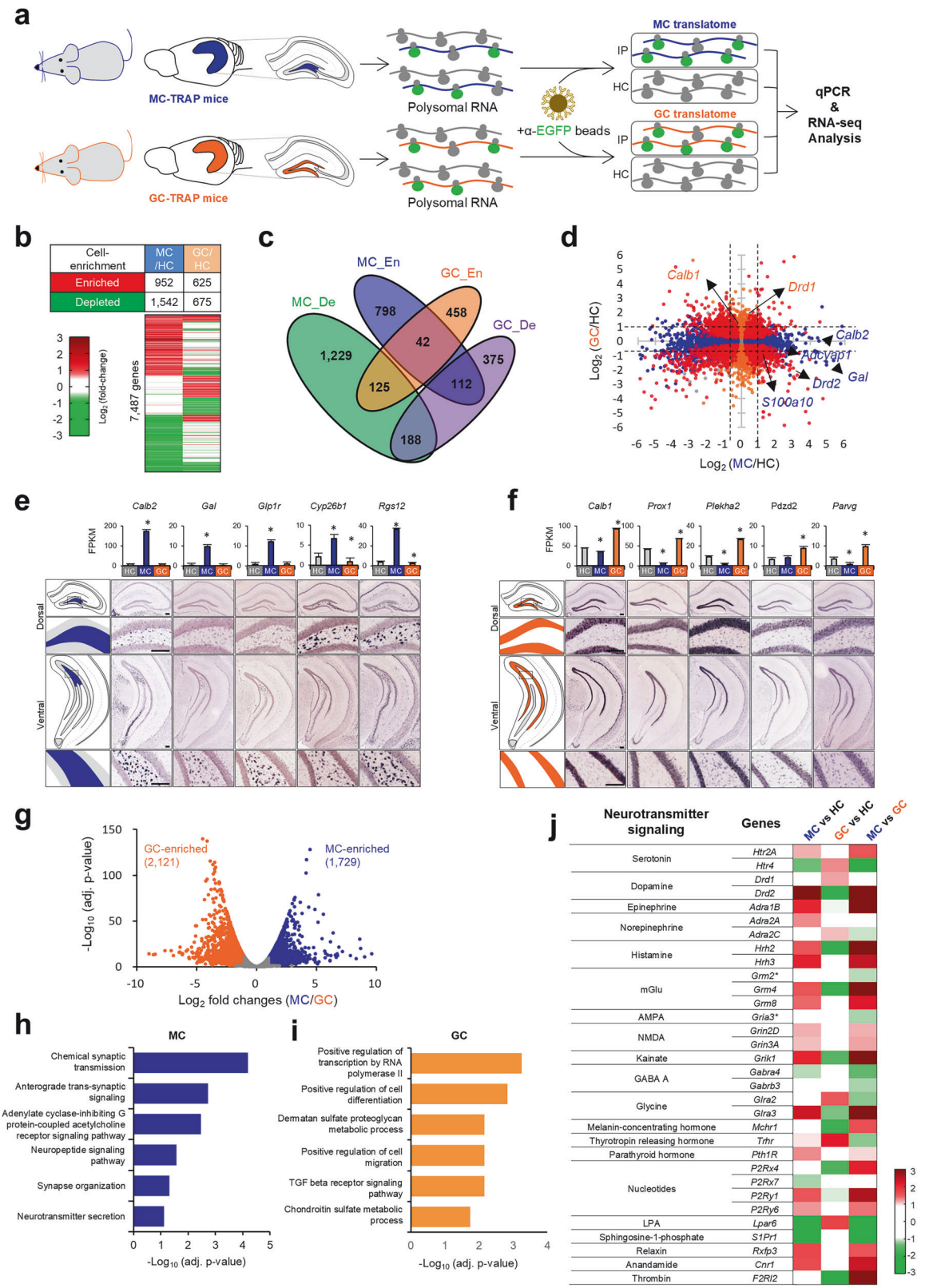

controls (HC) (Fig. 3d). These results highlight the enhanced sensitivity of the TRAP-seq approach for detecting cell type-specific translatomic responses to pharmacotherapy.

We next examined the biological pathways affected by chronic FLX treatment. Elevated serotonin levels during chronic SSRI treatment differentially influence the neuroplasticity of individual neuronal subtypes through selective activation of serotonin receptors [50]. Notably, multiple subtypes of serotonin receptors are differentially expressed in MCs and GCs, but their translations do not exhibit any observable changes with chronic FLX treatment

Fig. 2 Distinct translational profiles of GCs and MCs. a Schematic of the experiment paradigm. Purification of MC and GC translatome from hippocampal homogenates of MC-, GC-TRAP mice, respectively, followed by q-PCR and RNA-seq analysis (all male mice; MC-TRAP, $n = 6$; GC-TRAP, $n = 4$). **b** Heatmap showing genes enriched in MC or GC translatome versus hippocampal homogenate controls (HC). **c** Van diagram depicting the number of enriched or depleted genes of GCs or MCs. **d** Scatter plot of 9-quadrant diagram of translatome expression patterns in MCs and GCs. GC enriched genes are marked in red, and MC enriched genes are marked in blue. (**e** and **f**) Bar graph showing the FPKM value for individual gene enriched in MC-translatome or GC-translatome (top) and its representative ISH images at dorsal and ventral DG from Allen Brain Atlas (bottom). **g** Volcano plot depicting differentially translated genes in MC or GC translatome. Orange dots represent genes expressed in MC translatome, while blue dots represent genes with higher expression levels in GC translatome. DEGs were identified based on an adjusted p-value < 0.05 and an absolute $\log_2$ fold-change > 0.58 (corresponding to a 1.5-fold change).(**h and i**) Gene ontology enrichment analysis of biological processes for up-regulated genes in MC- or GC-translatome. **j** Heatmap comparing the log fold change of neurotransmitter signaling between MC and HC or GC and HC or MC and GC. Data are represented as means ± SEM. Pair-wise comparison by post hoc test; *p < 0.05, HC, hippocampal homogenate controls; MC, mossy cells; GC, granule cells, See also Figure S3 and Table S1.

(Fig. S5). In sharp contrast, a wide range of neuroplasticity-associated genes are translationally regulated in a cell type-specific manner. Of the genes upregulated by FLX in MCs (930 genes) and GCs (951 genes), only a small fraction (135 genes) overlapped between these two cell types, underscoring the distinct cellular responses (Fig. 3e, f, Table S2). We categorized these genes into three groups: (I) genes exclusively up-regulated in MCs (695), (II) genes exclusively up-regulated GCs (785), and (III) genes commonly up-regulated in both MCs and GCs (135). We then examined their enriched functions using GOBP pathway analysis (Fig. 3g – i, Table S2). The first subset of genes from the MC translatome was highly associated with 'peptide hormone processing' (Fig. 3g), while the second one from the GC translatome, 'synapse assembly' was highly enriched (Fig. 3h). The third group, commonly up-regulated by FLX in both cell types were highly enriched in 'cell adhesion' and 'modulation of synaptic transmission' (Fig. 3i). We further performed a direct comparison between the biological pathways augmented in MCs and those in GCs, based on GOBP and KEGG pathway analysis (Fig. 3j, k). This helps delineate the relative differences in the ways MCs and GCs undergo adaptive changes to chronic drug administration. In MCs, FLX treatment augments neuronal processes such as neuronal connectivity, synaptic transmission, ion transport, and action potential, whereas in GCs, metabolic processes, including glycolysis, lipid metabolism, and endocytosis, are prominent (Fig. 3j, k, Table S2). Critically, the neuropeptide signaling pathway in GOBP analysis and neuroactive ligand-receptor interactions in KEGG analysis emerged as key pathways induced by the chronic FLX treatment.

Further analysis of this finding revealed that chronic FLX triggers a coordinated remodeling of the DG's peptidergic signaling network at the translational level. Specifically, we found that many neuropeptide ligands, including *Adcyap1*, *Cck*, *Gal*, and *Nmb*, were enriched in MCs, with a tendency to be further increased by FLX treatment (Fig. 3l, Table S3). In addition, *Penk* was enriched in GCs and upregulated in response to FLX treatment. Concurrently, we observed a cell type-specific distribution of their cognate receptors, such as *Adcyap1r1* in GCs and other neuromodulatory receptors (*Cckbr, Nmbr, Pord1, Glp1r*) in MCs. We further confirmed that basal expression profiles of these neuropeptides and their receptors were consistent with ISH images from the mouse brain database of the Allen Brain Atlas (Fig. S6). Taken together, these data demonstrate that chronic FLX treatment initiates a comprehensive translatomic reprogramming of the DG peptidergic circuitry. This profound remodeling of key neuromodulatory pathways provides a direct molecular substrate for investigating how this circuit controls antidepressant efficacy.

Translational control of a neuropeptide PACAP in response to chronic FLX treatment

Our translatomic analysis revealed that chronic FLX treatment significantly remodels peptidergic signaling pathways, particularly in MCs (Fig. 3j – l). Among the various neuropeptides enriched in MCs, we prioritized PACAP (encoded by *Adcyap1*), because our TRAP-seq data showed it was significantly upregulated by chronic FLX treatment (Fig. S6a). This focus was further supported by distribution of its cognate receptor, PAC1 (encoded by *Adcyap1r1*), which is abundantly expressed in both GCs and MCs (Fig. S6a). This anatomical arrangement suggests a signaling network involving both paracrine (MC-to-GC) and potential autocrine (MC-to-MC) regulation within the DG circuitry. Consistent with this notion, the potential for PACAP to directly modulate GC activity has been previously reported [51]. Moreover, the PACAP system is well-implicated in stress responses and psychiatric disorders such as MDD and PTSD, underscoring its high clinical relevance [52, 53]. Taken together, these convergent lines of evidence prompted us to investigate the specific contribution of MC-derived PACAP signaling to the neuroplastic and behavioral effects of chronic FLX treatment.

Initially, we assessed the expression levels of PACAP and its cognate receptor, PAC1 receptors, using various methods. Using cell type-specific TRAP DTG analysis, we identified significant enrichment of *Adcyap1* in MCs relative to both the whole hippocampal tissue and GCs (Fig. S7a). Furthermore, we observed high expression levels of *Adcyap1r1*, primarily in GCs and to a lesser degree in MCs (Fig. S7b). Using in-situ hybridization (ISH), we then confirmed the exclusive localization of *Adcyap1* transcripts in the hilus where MCs are located and observed widespread distribution of *Adcyap1r1* transcripts in the granule cell layer where GCs are densely packed, as well as in the hilus (Fig. S7c, S7d). Moreover, we noted a dorsoventral difference of *Adcyap1* expression, with significantly higher levels in the ventral hilus compared to the dorsal region, although no significant differences were detected in *Adcyap1r1* expression levels along the dorsoventral axis (Fig. S7c, S7d). This expression pattern does not significantly differ based on sex (Fig. S7c–S7f). Through these results, we confirmed that the PACAP ligand and its receptor exhibit a high degree of cell type specificity across the dorsoventral axis of the DG.

Next, we proceeded to investigate the regulatory mechanisms of the *Adcyap1* gene in response to drug treatment, focusing on potential transcriptional and translational changes (Fig. 4a). Our TRAP analysis revealed that chronic FLX administration enhances the association of *Adcyap1* mRNA with EGFP-tagged ribosomal complex in MCs (Fig. 4b). To determine whether this increase was due to transcriptional upregulation, we employed quantitative PCR (qPCR) and in situ hybridization (ISH) to assess mRNA levels in the DG. Surprisingly, these analyses showed no significant increase in *Adcyap1* transcript levels following chronic FLX treatment (Fig. 4c, d, e). However, despite the stable mRNA levels, Western blot experiments demonstrated a marked elevation in PACAP protein expression after chronic FLX administration (Fig. 4f, g, S8). Interestingly, we observed that the regulation of *Adcyap1*/PACAP in response to chronic FLX treatment is consistent in both male and female mice (Fig. 4c – g). Collectively, our findings suggest that PACAP and its receptor display cell type-specific expression patterns within the DG, and PACAP undergoes cell type-specific translational control, rather than transcriptional regulations, in MCs as a response to chronic FLX treatment (Fig. 4h).

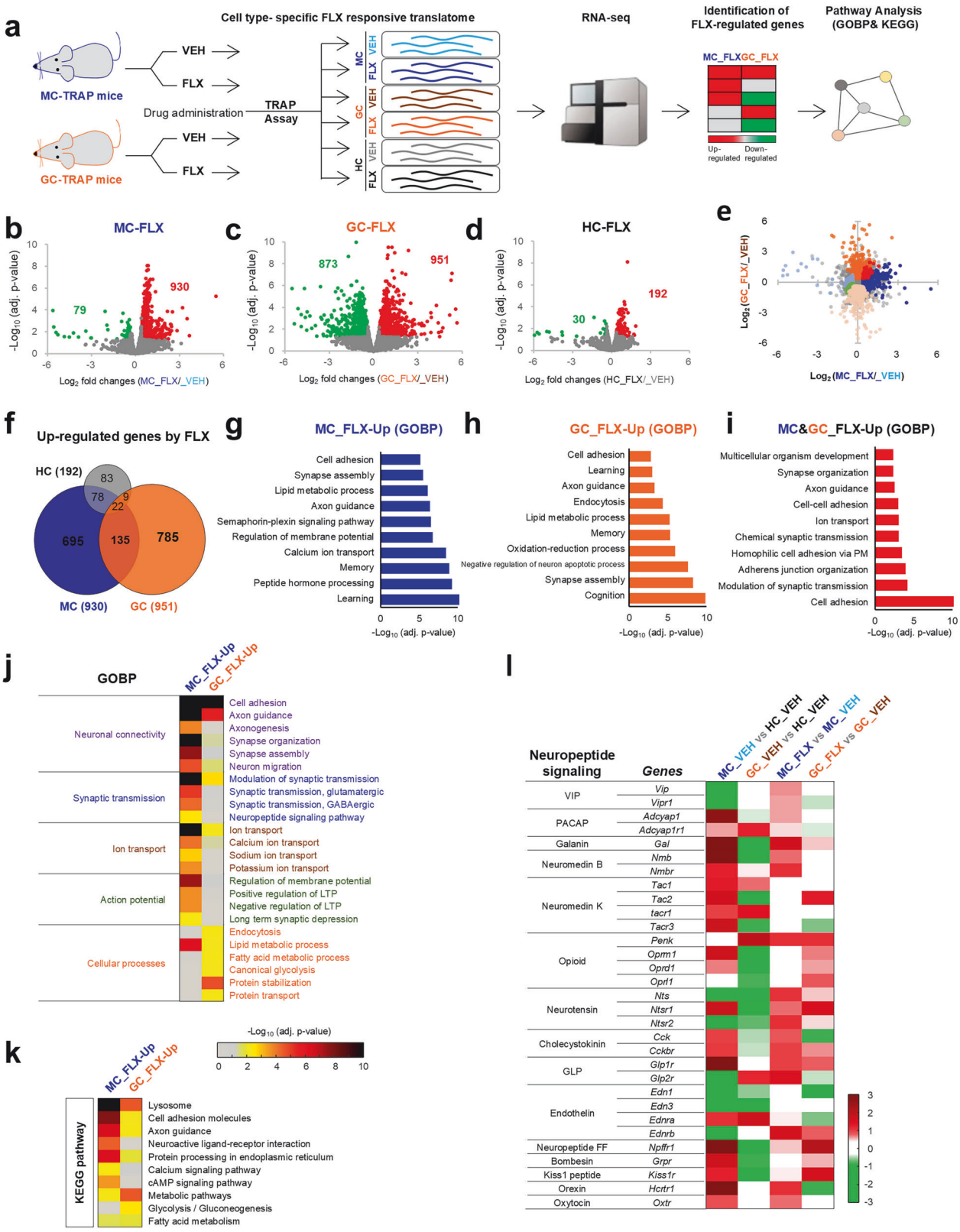

Regulation of antidepressant responses by PACAP expression in MCs

Next, we investigated whether PACAP depletion in MCs could affect neuroplastic changes and behavioral responses to chronic FLX administration, using chronically stressed animals to evaluate the therapeutic relevance of our findings in a disease model. Given known sex differences in PACAP function and its interactions with sex hormones [54–56], we conducted a comparative analysis between male and female mice.

Fig. 3 Cell type-specific translational responses to chronic FLX treatment. a Schematic illustration of the experiment paradigm for cell type-specific translatome comparison between MCs and GCs in stress-naïve animals (all male mice; HC:VEH, $n = 6$; HC:FLX, $n = 7$; MC-TRAP:VEH, $n = 6$; MC-TRAP:FLX, $n = 7$; GC-TRAP:VEH, $n = 4$; GC-TRAP:FLX, $n = 4$). (**b–d**) Volcano plot depicting significant differences between VEH and FLX in MC-TRAP or GC-TRAP or unbound sample. Log_2 (Fold change) values > 0 (red) indicate increase, and those < 0 (green) decrease. **e** Scatter plot of 4-quadrant diagram of translatome expression patterns in MCs and GCs by chronic FLX treatment. GC enriched and depleted genes are marked in red group color, and MC enriched and depleted genes are marked in blue group color. **f** Van diagram depicting the number of up-regulated genes by FLX in MCs, GCs or HC. (**g–i**) The top 10 up-regulated biological processes by chronic FLX treatment in MCs, GCs, or in both MCs and GCs. **j** Gene ontology enrichment analysis of biological processes for upregulated genes by chronic FLX administration in MC or GC. **k** KEGG pathway analysis of up-regulated mRNA in MCs and GCs by chronic FLX treatment. The vertical axis represents the pathway category, and the horizontal axis represents the enrichment score [-log(*p*-value)] of the pathway. **l** Heatmap comparing the log fold change of neuropeptide signaling by chronic FLX treatment on MCs, GCs and HC. HC, hippocampal homogenates; MC, mossy cells; GC, granule cells; VEH, vehicle; FLX, fluoxetine, See also Table S2, and S3, Figure S4, S5, and S6.

We established an animal model with PACAP depletion in ventral MCs. Control (shRluc-EGFP) or *Adcyap1* knockdown (sh-*Adcyap1*-EGFP) AAV was locally injected into the ventral hilus, an area with higher *Adcyap1* expression compared to the dorsal part (Fig. S9a). Viral transduction of ventral MCs was confirmed by EGFP-labeled somas in the hilus of the ventral DG and their axonal fibers in the inner molecular layer of the dorsal DG (Fig. S9b). AAV injection significantly reduced *Adcyap1* mRNA in hilar MCs without affecting *Adcyap1r1* expression in the granule cell layer (Fig. S9c–S9e). To first characterize the basal behavioral phenotype of the ventral hilus-targeted *Adcyap1* KD, we subjected a cohort of non-stressed, untreated mice to a battery of tests for anxiety-like behavior and locomotion (Fig. S10a). While basal locomotion remained unaffected in the open field test (Fig. S10b, S10c). *Adcyap1* KD elevated anxiety-like behaviors in the light-dark box and elevated plus maze tests, prominently in female mice (Fig. S10d, S10e).

Having characterized the basal phenotype, we next determined if PACAP signaling was required for the therapeutic effects of FLX in chronically stressed animals. Following a 2-week restraint stress period and 3 weeks of VEH or FLX treatment (15 mg/kg/day), control or *Adcyap1* KD mice were subjected to novelty-suppressed feeding (NSF) and tail-suspension tests (TST), standard assays of antidepressant-like effects in rodents [57, 58] (Fig. 5a). In the NSF test, FLX-induced behavioral changes are abolished by ventral hilus-targeted *Adcyap1* KD in females (Fig. 5b-female). In contrast, male groups exhibit comparable reductions in feeding latency with FLX regardless of *Adcyap1* KD (Fig. 5b-male). In the TST, chronic FLX treatment attenuates behavioral despair in both sexes, with *Adcyap1* KD impairing this effect prominently in females (Fig. 5c). Notably, chronic FLX treatment do not alter general locomotor activity of female mice as measured in the open field arena, indicating that the observed behavioral changes in the NSF and TST are unlikely to be confounded by aberrant alterations in basal locomotion (Fig. S11).

We next examined adult hippocampal neurogenesis, a hallmark of chronic antidepressant action in the DG [28, 59] (Fig. 5d). To capture both proliferating and immature neuronal populations, we analyzed BrdU incorporation (tagged 3 h prior to sacrifice) together with DCX immunolabeling. FLX-induced cell proliferation (cytogenesis) remains unaltered in males but is abolished specifically in *Adcyap1* KD females as compared to controls (Fig. 5e, f) In males, FLX treatment showed a marginal attenuation of DCX-related effects by *Adcyap1* KD, whereas no effect of *Adcyap1* KD was observed on BrdU incorporation by chronic FLX. In contrast, in females, the effects of FLX treatment were abolished by *Adcyap1* KD in both DCX and BrdU measures (Figs. 5e – h).

Chronic FLX administration has been shown to suppress the activity-dependent induction of IEGs in GCs in response to aversive stimuli [33, 34]. This suppression is attributed to altered neuroplasticity in the neural circuit, which is associated with behavioral outcomes following chronic SSRI treatment [33, 34]. Post-FLX treatment, mice were exposed to an aversive stimulus, tail suspension and then subjected to immuno-histological analysis for IEGs such as Arc and c-fos (Fig. 5i). Notably, chronic FLX administration suppresses GC IEG induction in response to aversive stimuli, which is abolished by *Adcyap1* KD in MCs. This PACAP-dependent suppression of IEGs induction is evident only in female, but not male, mice (Fig. 5j, k, S11a, S11b).

Collectively, PACAP regulation in MCs plays a crucial role in the neuroplastic and behavioral changes in response to chronic FLX treatment. These PACAP-dependent antidepressant actions are prominent in female mice, highlighting sex differences in antidepressant responses.

DISCUSSION

SSRIs exert their therapeutic effects through long-term neuroplastic changes, which are underpinned by alterations in gene transcription and protein translation. Our study reveals that chronic fluoxetine (FLX) treatment selectively enhances translational activity in specific neuronal populations within the DG. We conducted a comprehensive analysis of the cell type-specific translatome in the DG, with a particular focus on MCs and GCs following prolonged antidepressant administration. Our findings demonstrate distinct translatomic profiles between MCs and GCs, both at baseline and in response to chronic FLX treatment. Notably, we observed an enrichment of multiple neuropeptides in MCs, with their translation further upregulated following chronic FLX exposure. Among these, we identified PACAP as a key player mediating FLX-induced neuroplastic changes in the DG and subsequent behavioral outcomes prominently in female mice. These results underscore the importance of cell type-specific translational regulation of PACAP as a core component of the antidepressant mechanism of action in females.

FLX regulation of cell type-specific translation in the DG

Protein translation is strongly associated with various mental illnesses as well as their therapeutic recovery, possibly through its crucial involvement in neuroplasticity control [13]. Particularly, previous reports have emphasized its significance within specific brain regions, such as the hippocampus and prefrontal cortex in the pathology of MDD and antidepressant response [12, 15, 16, 60]. These studies have demonstrated the essential involvement of the mechanistic target of rapamycin (mTOR) signaling pathway, a key indicator of translational control, in mediating the long-term effects of SSRIs and ketamine [15, 16, 61–63]. Previous reports extensively implicate two glutamatergic neurons, MCs and GCs comprising the DG circuitry, in antidepressant response [24, 26, 29, 33]. In the present study, when comparing the impact of chronic FLX treatment on individual cell type based on the phosphorylation levels of ribosomal S6 protein, an increase was observed only in MCs, while no significant changes were observed in GCs, indicating that the level of translational activity induced by the antidepressant is cell type-specific manner.

The differential mechanisms of translational regulation between the two cell types in response to antidepressants remain unclear.

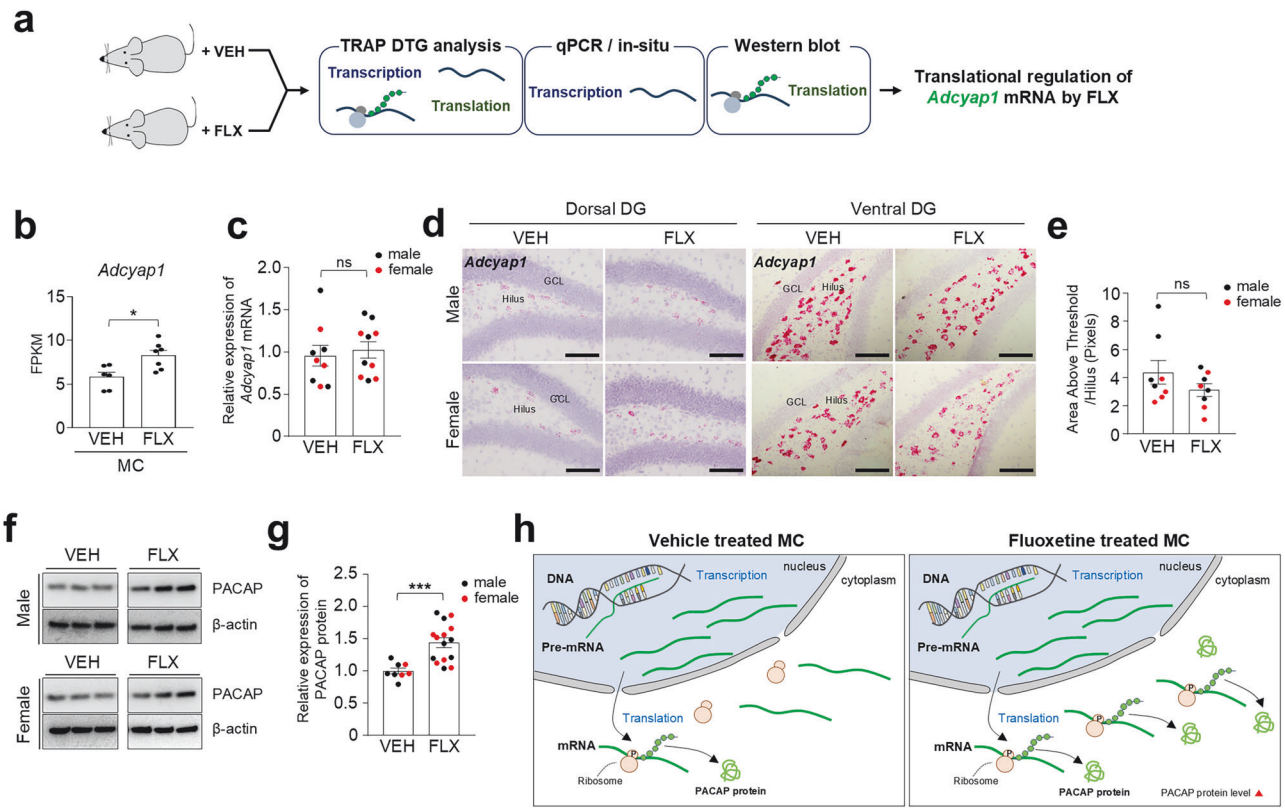

Fig. 4 Translational induction of MC-enriched neuropeptide PACAP by chronic FLX treatment. a Schematic illustration of the experimental paradigm. VEH or FLX (15 mg/kg/day) were administered for 2 weeks in stress-naïve animals prior to a series of analyses as indicated. **b** Comparison of the *Adcyap1* expression levels (by FPKM values) in MCs between vehicle (VEH) and fluoxetine (FLX) treated mice. Two-tailed, unpaired *t*-test; $p = 0.0109$ (all male mice; VEH, $n = 6$; FLX, $n = 7$). **c** Quantification of relative expression of *Adcyap1* in hippocampus by chronic FLX treatment using qPCR analysis. Two-tailed, unpaired *t*-test; $p = 0.6640$ (VEH:Male, $n = 5$; VEH:Female, $n = 4$; FLX:Male, $n = 5$; FLX:Female, $n = 5$). **d** Representative images of chromogenic ISH staining for *Adcyap1*-RNA (Red) on VEH-treated or FLX-treated mice. Scale bar; 100 μm. **e** Quantification of *Adcyap1*-positive fluorescence in hilus region following chronic antidepressant treatment. Two-tailed, unpaired *t*-test; $p = 0.2048$ (VEH:Male, $n = 4$; VEH:Female, $n = 4$; FLX:Male, $n = 4$; FLX:Female, $n = 4$). **f** Western blot assay demonstrates that fluoxetine (FLX) treatment increased PACAP protein levels in hippocampus. **g** Quantification of relative expression of PACAP in hippocampus by chronic FLX treatment using western blot analysis. Two-tailed, unpaired *t*-test; $p = 0.0007$ (VEH:Male, $n = 4$; VEH:Female, $n = 3$; FLX:Male, $n = 7$; FLX:Female, $n = 8$). **h** Illustration depicting the differences in translating mRNA between VEH-treated and FLX-treated mice. Data are represented as means ± SEM. Student's *t*-test, *p < 0.05, ***p < 0.001, ns, non-significant. VEH, vehicle; FLX, fluoxetine. See also Figure S7 and S8.

However, intriguingly, according to our TRAP RNA-seq results, serotonin receptor subtypes are differentially expressed in both cell types, and this expression pattern is consistent with the histological results from the Allen Brain Atlas. Specifically, serotonin receptors such as *Htr1a* and *Htr4* are enriched in GCs, and the significance of these receptors in response to antidepressant drugs has already been reported [29, 64]. Additionally, we also confirmed that *Htr2a* is highly enriched in MCs. Thus, these differences in serotonin receptor expression might be associated with the distinct translational regulation by sustained serotonin levels alongside chronic FLX treatment.

Our TRAP-seq data revealed that Chronic FLX treatment significantly altered the translational landscape in both MCs and GCs, with a marked increase in neuroplasticity-associated biological pathways. Although these DG cell types are known to exhibit inherent transcriptional differences at baseline, our findings provide a unique perspective by delineating the specific translatomic profiles engaged by FLX in each population. This differential translation not only underscores the expected divergence in translational profile but also identifies novel cell type-specific pathways that may differentially contribute to DG function and behavioral outcomes. Specifically, MC-upregulated genes are associated with peptide hormone processing, calcium ion transport, and synaptic assembly, whereas GC-upregulated genes are linked to synapse assembly, and lipid metabolic processes in biological pathway analysis. Minimal overlap existed between MCs and GCs, underscoring cell type-specific translational changes underlying antidepressant responses. Collectively, these findings indicate that rather than eliciting uniform molecular response, chronic FLX treatment remodels translational programs with the DG in a cell type-specific manner.

Translational reprogramming of the DG peptidergic circuitry by chronic FLX treatment

Neuropeptides are essential neuromodulators that regulate neural circuits to allow for behavioral flexibility and plasticity-processes critical for adapting to environmental change [65]. In this context, a critical finding from our translatomic analysis was the profound and coordinated remodeling of the DG peptidergic circuitry by chronic FLX treatment. This is particularly significant given the extensive evidence implicating neuropeptide systems in the mechanism of antidepressant actions [66, 67].

Building on this framework, our TRAP RNA-seq dataset reveals a multi-faceted reprogramming of neuropeptide systems, including both ligands and receptors at the translational level. In MCs, we observed an cell type-specific enrichment and FLX-induced upregulation of numerous neuropeptide ligands, including *Adcyap1* [68],*Gal* [69] and *Cck* [70, 71], all of which have been independently linked to depression and antidepressant response. Concurrently, the translatomes of DG cell types showed a

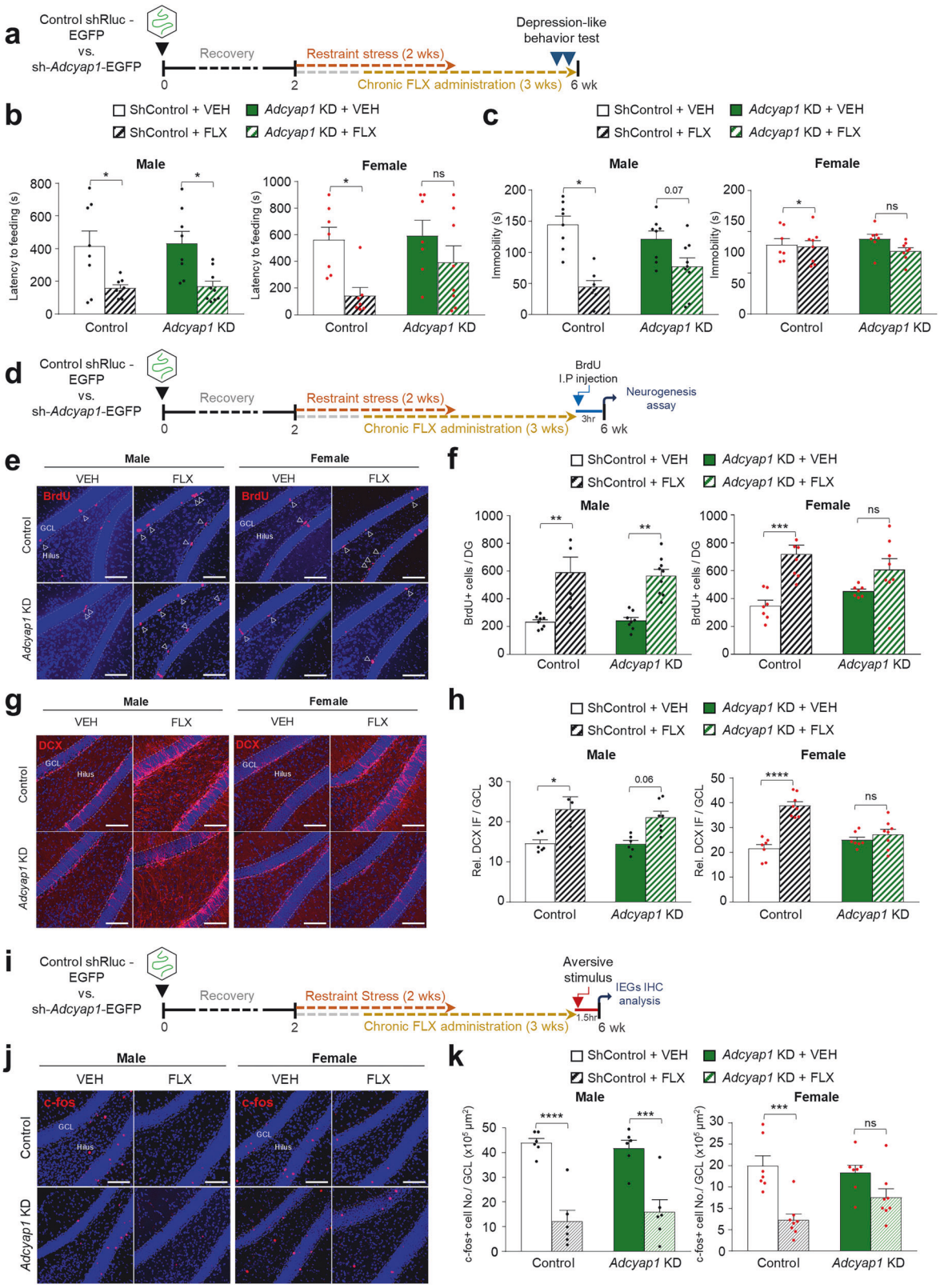

coordinated upregulation of cognate receptor for various neuropeptide. For example, receptors for mood-regulating peptides like *Cckbr* [72], *Glp1r* [73] and *Oxtr* [74] were increased in MCs, while opioid receptors like *Oprm1*, and *Oprd1* [75] were upregulated in GCs, by chronic FLX treatment. Notably, these findings raise the possibility that FLX may enhance not only local neuropeptidergic signaling but also long-range neuromodulatory pathways, with MCs and GCs potentially acting as distinct targets or integration hubs for peptidergic inputs form distant brain regions. For example, the FLX-induced upregulation of *Glp1r* in MCs could

Fig. 5 Sex-specific antidepressant responses modulated by ventral hilus-targeted *Adcyap1* KD. a Experimental design. Control shRluc-EGFP-injected or Sh-*Adcyap1*-EGFP-injected mice were subjected to restraint stress for 2 weeks, concurrently administrated VEH or FLX for 3 weeks. **b** The latency to feeding after a day of fasting in novelty-suppressed feeding test. For male; Control:VEH, $n = 8$; Control:FLX, $n = 8$; *Adcyap1*KD:VEH, $n = 8$; *Adcyap1*KD:FLX, $n = 9$, Two-way ANOVA, [*Adcyap1* KD × drug interaction $F(1,29) = 0.003794$; $p = 0.9513$, *Adcyap1* KD $F(1,29) = 0.04669$; $p = 0.8304$, drug $F(1.29) = 17.9$; $p = 0.0002$], followed by the Tukey's post hoc test. Tukey's multiple comparisons test [Control:VEH vs. Control:FLX; $p = 0.0331$, *Adcyap1* KD:VEH vs. *Adcyap1* KD:FLX; $p = 0.0221$] For female; Control:VEH, $n = 7$; Control:FLX, $n = 8$; *Adcyap1*KD:VEH, $n = 7$; *Adcyap1*KD:FLX, $n = 8$, Two-way ANOVA, [*Adcyap1* KD × drug interaction $F(1,25) = 1.089$; $p = 0.3067$, *Adcyap1* KD $F(1,25) = 1.858$; $p = 0.1850$, drug $F(1.25) = 8.928$; $p = 0.0062$], followed by the Tukey's post hoc test. Tukey's multiple comparisons test [Control:VEH vs. Control:FLX; $p = 0.0444$, *Adcyap1* KD:VEH vs. *Adcyap1* KD:FLX; $p = 0.5124$] **c** Tail suspension test after chronic treatment of VEH or FLX. For male; Control:VEH, $n = 8$; Control:FLX, $n = 7$; *Adcyap1*KD:VEH, $n = 8$; *Adcyap1*KD:FLX, $n = 9$, Two-way ANOVA, [*Adcyap1* KD × drug interaction $F(1,28) = 4.59$; $p = 0.0410$, *Adcyap1* KD $F(1,28) = 0.1295$; $p = 0.7217$, drug $F(1.28) = 31.26$; $p < 0.0001$], followed by the Tukey's post hoc test. Tukey's multiple comparisons test [Control:VEH vs. Control:FLX; $p < 0.0001$, *Adcyap1* KD:VEH vs. *Adcyap1* KD:FLX; $p = 0.0786$] For female; Control:VEH, $n = 6$; Control:FLX, $n = 6$; *Adcyap1*KD:VEH, $n = 6$; *Adcyap1*KD:FLX, $n = 6$, Two-way ANOVA, [*Adcyap1* KD × drug interaction $F(1,20) = 2.756$; $p = 0.1125$, *Adcyap1* KD $F(1,20) = 0.2665$; $p = 0.6114$, drug $F(1.20) = 8.83$; $p = 0.0075$], followed by the Tukey's post hoc test. Tukey's multiple comparisons test [Control:VEH vs. Control:FLX; $p = 0.0183$, *Adcyap1* KD:VEH vs. *Adcyap* KD:FLX; $p = 0.7907$]. **d** Experimental design. All the animals were labeled with BrdU for the last 3 h prior to perfusion. **e** Representative images with α-BrdU immunostaining results of male and female mice. BrdU+ cells in the subgranular zone (SGZ) were counted. Scale bars, 100 μm. **f** Quantification of BrdU-positive cells in the SGZ of male and female mice. For male; Control:VEH, $n = 8$; Control:FLX, $n = 8$; *Adcyap1*KD:VEH, $n = 8$; *Adcyap1*KD:FLX, $n = 9$, Two-way ANOVA, [*Adcyap1* KD × drug interaction $F(1,29) = 0.06755$; $p = 0.7968$, *Adcyap1* KD $F(1,29) = 0.01472$; $p = 0.9043$, drug $F(1.29) = 31.57$; $p < 0.0001$], followed by the Tukey's post hoc test. Tukey's multiple comparisons test [Control:VEH vs. Control:FLX; $p = 0.0016$, *Adcyap1* KD:VEH vs. *Adcyap1* KD:FLX; $p = 0.0032$]. For female; Control:VEH, $n = 7$; Control:FLX, $n = 8$; *Adcyap1*KD:VEH, $n = 7$; *Adcyap1*KD:FLX, $n = 8$, Two-way ANOVA, [*Adcyap1* KD × drug interaction $F(1,25) = 7.487$; $p = 0.0083$, *Adcyap1* KD $F(1,25) = 0.008169$; $p = 0.9283$, drug $F(1.25) = 44.27$; $p < 0.0001$], followed by the Tukey's post hoc test. Tukey's multiple comparisons test [Control:VEH vs. Control:FLX; $p = 0.0007$, *Adcyap1* KD:VEH vs. *Adcyap1* KD:FLX; $p = 0.3544$] **g** Representative image of postmitotic immature neurons labeled with α-Doublecortin (DCX; red). Scale bars, 100 μm. **h** Quantification of relative DCX immunofluorescence intensity (Rel. DCX IF) in subgranular and granular zone of male and female mice. For male; Control:VEH, $n = 6$; Control:FLX, $n = 6$; *Adcyap1*KD:VEH, $n = 6$; *Adcyap1*KD:FLX, $n = 7$, Two-way ANOVA, [*Adcyap1* KD × drug interaction $F(1,21) = 0.2759$; $p = 0.6049$, *Adcyap1* KD $F(1,21) = 0.3437$; $p = 0.5640$, drug $F(1.21) = 18.03$; $p = 0.0004$], followed by the Tukey's post hoc test. Tukey's multiple comparisons test [Control:VEH vs. Control:FLX; $p = 0.0161$, *Adcyap1* KD:VEH vs. *Adcyap1* KD:FLX; $p = 0.0621$]. For female; Control:VEH, $n = 7$; Control:FLX, $n = 8$; *Adcyap1*KD:VEH, $n = 7$; *Adcyap1*KD:FLX, $n = 8$, Two-way ANOVA, [*Adcyap1* KD × drug interaction $F(1,26) = 20.23$; $p = 0.0001$, Adcyap1 KD $F(1,26) = 5.864$; $p = 0.0230$, drug $F(1.26) = 34.52$; $p < 0.0001$], followed by the Tukey's post hoc test. Tukey's multiple comparisons test [Control:VEH vs. Control:FLX; $p < 0.0001$, *Adcyap1* KD:VEH vs. *Adcyap1* KD:FLX; $p = 0.7654$]. **i** Experimental design. All the animals received an aversive stimulus 1.5 h prior to perfusion. **j** Representative IHC images of c-fos-positive cells (red) with counter staining (blue, DraQ5) in the control of *Adcyap1* KD male or female mice and further treated with either saline or fluoxetine. Scale bar, 100μm. **k** Quantitation of c-fos-positive cell number. For male; Control:VEH, $n = 6$; Control:FLX, $n = 6$; *Adcyap1*KD:VEH, $n = 6$; *Adcyap1*KD:FLX, $n = 6$, Two-way ANOVA, [*Adcyap1* KD × drug interaction $F(1,20) = 0.6132$; $p = 0.4427$, *Adcyap1* KD $F(1,20) = 0.04902$; $p = 0.8270$, drug $F(1.20) = 56.45$; $p < 0.0001$;], followed by the Tukey's post hoc test. Tukey's multiple comparisons test [Control:SAL vs. Control:FLX; $p < 0.0001$, *Adcyap1* KD:SAL vs. *Adcyap1* KD:FLX; $p = 0.0006$]. For female; Control:VEH, $n = 7$; Control:FLX, $n = 8$; *Adcyap1*KD:VEH, $n = 7$; *Adcyap1* KD:FLX, $n = 8$, Two-way ANOVA, [*Adcyap1* KD × drug interaction $F(1,26) = 3.319$; $p = 0.0800$, *Adcyap1* KD $F(1,26) = 0.9471$; $p = 0.3394$, drug $F(1,26) = 23.48$; $p < 0.0001$], followed by the Tukey's post hoc test. Tukey's multiple comparisons test [Control:SAL vs. Control:FLX; $p = 0.0004$, *Adcyap1* KD:SAL vs. *Adcyap1* KD:FLX; $p = 0.1677$] Data are represented as means ± SEM. Pair-wise comparison; *p < 0.05, **p < 0.01, ***p < 0.001, ****p < 0.0001, ns, non-significant. GCL, granule cell layer; DG, dentate gyrus; VEH, vehicle; FLX, fluoxetine. See also Figure S9, S10, S11 and S12.

reflect heightened sensitivity to long-range GLP-1 inputs, while the increased expression of *Gal*, a ligand known to modulate serotonin transmission [69, 76], may likewise indicate the engagement of long-range peptidergic modulation.

This widespread and cell type-specific remodeling suggests that chronic FLX treatment progressively reshapes the neuromodulatory landscape of the DG. This reprogramming may enhance the circuit's sensitivity to both local peptidergic communication within the DG and long-range inputs from other brain regions, priming specific dentate cell types to better integrate mood-regulating signals. By enhancing the translational efficiency of these key signaling molecules, the antidepressant appears to bolster the circuit's capacity for adaptation, a process fundamental to its therapeutic effect on mood.

A neuropeptide PACAP in MCs as a female-specific mediator of antidepressant actions in female mice

PACAP, a versatile neuropeptide acting through receptors like PAC1, VPAC1 and VPAC2, modulates synaptic plasticity and behavioral flexibility [77–79]. Research indicates its involvement in stress responses [80–82], and its disruption is linked to stress-related psychiatric disorders such as MDD and post-traumatic stress disorder (PTSD) [68, 83–86]. Notably, these disorders exhibit a significant sex bias, with female being more vulnerable [87–89]. A growing body of evidence specifically links the PACAP system to this sex difference. Human studies have demonstrated a sex-specific association between PACAP, and its PAC1 receptors, and PTSD symptoms in women [54, 90]. Mechanistically, the gene promoter for PAC1 receptor (encoded by *Adcyap1r1*) contains the *estrogen response elements* (ERE), and *Adcyap1* variants, located in the ERE are more strongly associated with female PTSD patients [54, 90]. In addition, preclinical study has shown that administering estrogen to ovariectomized rats increases the expression of both *Adcyap1* and *Adcyap1r1* [54], suggesting a significant interaction between estrogen and the PACAP system.

Our findings provide a direct functional link between this sex-specific PACAP system and the efficacy of FLX treatment. We demonstrated that in chronically stressed female mice, the therapeutic actions of chronic FLX were abolished by the ventral hilus-targeted depletion of PACAP. Specifically, this PACAP depletion only in female mice cancels the ability of FLX to suppress aberrant GC activation (IEG induction) in response to aversive stimuli, a phenomenon associated with the behavioral outcomes of chronic SSRI treatment [33, 34]. Furthermore, chronic SSRI administration induces the generation of new GCs in the DG, contributing to stress resilience and the beneficial actions of antidepressants [27, 28, 59, 91]. Interestingly, the proneurogenic effects of the drug is abolished in female mice with the ventral hilus-targeted PACAP depletion, but remains unaffected in their male counterparts. Consistent with these neurobiological findings, the behavioral benefits of chronic FLX were also significantly attenuated in females, an effect not observed in male. This result is supported by other research showing that chemogenetic manipulation of MC activity produces sexually dimorphic behavioral

outcomes [92]. Together, our findings identify the cell type-specific translational control of PACAP as a crucial, sex-specific mechanism that gates the neuroplastic and behavioral efficacy of chronic antidepressant treatment in female mice.

In summary, our study establishes that translational reprogramming of neuropeptidergic circuits is a critical mechanism for the neuroplastic and behavioral effects of chronic FLX treatment. We demonstrated that FLX induces cell type-specific translational upregulation of PACAP in MCs, a mechanism that is essential for key neuroplastic changes in the DG and subsequent antidepressant-like behavioral responses. This effect was strikingly prominent in female mice, providing a novel framework for understanding sex-specific antidepressant efficacy. This insight advances our understanding of antidepressant action beyond transcriptional regulation, highlighting the crucial interplay between cell-specific translational control and neuroplasticity. These findings suggest new directions for targeted therapies, representing a significant contribution to neuropsychopharmacology.

Limitations of the study

The present study has several limitations. First, our evidence for the "translational control" mechanism has methodological constraints; we used prS6 as a proxy for translational activation and did not use direct genetic manipulations of the translational machinery to prove dependency. Second, our core translatomic discovery was conducted in stress-naïve animals. While this provided mechanistic clarity, these molecular signatures may not fully reflect a pathological state. Third, the biological specificity of our model is limited; the *Adcyap1* knockdown was not perfectly cell-specific, and our key findings in females did not account for the estrous cycle. Finally, our conclusions are based on a single antidepressant, fluoxetine, and may not generalize to other classes of antidepressants.

DATA AVAILABILITY

All data supporting the findings of this study are included in Article and its Supplementary Information. Source data and additional datasets generated and/or analyzed during this study are available from the corresponding author upon reasonable request. Sequencing data have been deposited in the NCBI Gene Expression Omnibus (GEO) under accession number GSE309750.

REFERENCES

1. Friedrich MJ. Depression is the leading cause of disability around the world. JAMA. 2017;317:1517–17. https://doi.org/10.1001/jama.2017.3826
2. Hervás I, Artigas F. Effect of fluoxetine on extracellular 5-hydroxytryptamine in rat brain. Role of 5-HT autoreceptors. Eur J Pharmacol. 1998;358:9–18. https://doi.org/10.1016/s0014-2999(98)00579-2
3. Stahl SM. Mechanism of action of serotonin selective reuptake inhibitors. Serotonin receptors and pathways mediate therapeutic effects and side effects. J Affect Disord. 1998;51:215–35. https://doi.org/10.1016/s0165-0327(98)00221-3
4. Harmer CJ, Duman RS, Cowen PJ. How do antidepressants work? new perspectives for refining future treatment approaches. Lancet Psychiat. 2017;4:409–18. https://doi.org/10.1016/S2215-0366(17)30015-9
5. Kraus C, Castren E, Kasper S, Lanzenberger R. Serotonin and neuroplasticity - Links between molecular, functional and structural pathophysiology in depression. Neurosci Biobehav Rev. 2017;77:317–26. https://doi.org/10.1016/j.neubiorev.2017.03.007
6. Cui L, Li S, Wang S, Wu X, Liu Y, Yu W, et al. Major depressive disorder: hypothesis, mechanism, prevention and treatment. Signal Transduct Target Ther. 2024;9:30. https://doi.org/10.1038/s41392-024-01738-y
7. Yao, V Aly A, Kalik S, Gresack J, Wang W, Handler A et al. Neuron-Glia signaling regulates the onset of the antidepressant response. *bioRxiv* 2021.2007.2023.453443 [Preprint]. (2021). Available from : https://www.biorxiv.org/content/10.1101/2021.07.23.453443v1.
8. Oh Y-S, Gao P, Lee KW, Ceglia I, Seo JS, Zhang X, et al. SMARCA3, a chromatin-remodeling factor, is required for p11-Dependent antidepressant action. Cell. 2013;152:831–43. https://doi.org/10.1016/j.cell.2013.01.014
9. Machado-Vieira R, Zanetti MV, Teixeira AL, Uno M, Valiengo LL, Soeiro-de-Souza MG, et al. Decreased AKT1/mTOR pathway mRNA expression in short-term bipolar disorder. Eur Neuropsychopharmacology. 2015;25:468–73. https://doi.org/10.1016/j.euroneuro.2015.02.002
10. Amorim IS, Kedia S, Kouloulia S, Simbriger K, Gantois I, Jafarnejad SM, et al. Loss of eIF4E Phosphorylation Engenders Depression-like Behaviors via Selective mRNA Translation. J Neurosci. 2018;38:2118–33. https://doi.org/10.1523/jneurosci.2673-17.2018
11. Zhou M, Li W, Huang S, Song J, Kim JY, Tian X, et al. mTOR Inhibition ameliorates cognitive and affective deficits caused by Disc1 knockdown in adult-born dentate granule neurons. Neuron. 2013;77:647–54. https://doi.org/10.1016/j.neuron.2012.12.033
12. Dwyer JM, Maldonado-Aviles JG, Lepack AE, DiLeone RJ, Duman RS. Ribosomal protein S6 kinase 1 signaling in prefrontal cortex controls depressive behavior. Proc Natl Acad Sci USA. 2015;112:6188–93. https://doi.org/10.1073/pnas.1505289112
13. Laguesse S, Ron D. Protein Translation and Psychiatric Disorders. Neuroscientist. 2020;26:21–42. https://doi.org/10.1177/1073858419853236
14. Aguilar-Valles A, Haji N, De Gregorio D, Matta-Camacho E, Eslamizade MJ, Popic J, et al. Translational control of depression-like behavior via phosphorylation of eukaryotic translation initiation factor 4E. Nat Commun. 2018;9:2459. https://doi.org/10.1038/s41467-018-04883-5
15. Liu XL, Luo L, Mu RH, Liu BB, Geng D, Liu Q, et al. Fluoxetine regulates mTOR signalling in a region-dependent manner in depression-like mice. Sci Rep. 2015;5:16024. https://doi.org/10.1038/srep16024
16. Xu D, Sun Y, Wang C, Wang H, Wang Y, Zhao W, et al. Hippocampal mTOR signaling is required for the antidepressant effects of paroxetine. Neuropharmacology. 2018;128:181–95. https://doi.org/10.1016/j.neuropharm.2017.10.008
17. Herzog DP, Pascual Cuadrado D, Treccani G, Jene T, Opitz V, Hasch A, et al. A distinct transcriptional signature of antidepressant response in hippocampal dentate gyrus granule cells. Transl Psychiatry. 2021;11:4 https://doi.org/10.1038/s41398-020-01136-2
18. Ibrahim EC, Gorgievski V, Ortiz-Teba P, Belzeaux R, Turecki G, Sibille E, et al. Transcriptomic studies of antidepressant action in rodent models of depression: a first meta-analysis. Int J Mol Sci. 2022;23:13453. https://doi.org/10.3390/ijms232113543
19. Hervé M, Bergon A, Le Guisquet AM, Leman S, Consoloni JL, Fernandez-Nunez N, et al. Translational identification of transcriptional signatures of major depression and antidepressant response. Front Mol Neurosci. 2017;10:248. https://doi.org/10.3389/fnmol.2017.00248
20. Cho J, Yu NK, Choi JH, Sim SE, Kang SJ, Kwak C, et al. Multiple repressive mechanisms in the hippocampus during memory formation. Science. 2015;350:82–7. https://doi.org/10.1126/science.aac7368
21. Sahay A, Hen R. Adult hippocampal neurogenesis in depression. Nat Neurosci. 2007;10:1110–5. https://doi.org/10.1038/nn1969
22. Schmaal L, Veltman DJ, van Erp TG, Sämann PG, Frodl T, Jahanshad N, et al. Subcortical brain alterations in major depressive disorder: findings from the ENIGMA major depressive disorder working group. Mol Psychiatry. 2016;21:806–12. https://doi.org/10.1038/mp.2015.69
23. Kobayashi K, Shikano K, Kuroiwa M, Horikawa M, Ito W, Nishi A, et al. Noradrenaline activation of hippocampal dopamine D1 receptors promotes antidepressant effects. Proc Natl Acad Sci. 2022;119:e2117903119. https://doi.org/10.1073/pnas.2117903119
24. Shuto T, Kuroiwa M, Sotogaku N, Kawahara Y, Oh YS, Jang JH, et al. Obligatory roles of dopamine D1 receptors in the dentate gyrus in antidepressant actions of a selective serotonin reuptake inhibitor, fluoxetine. Mol Psychiatr. 2020;25:1229–44. https://doi.org/10.1038/s41380-018-0316-x
25. Umschweif G, Greengard P, Sagi Y. The dentate gyrus in depression. Eur J Neurosci. 2021;53:39–64. https://doi.org/10.1111/ejn.14640
26. Oh SJ, Cheng J, Jang JH, Arace J, Jeong M, Shin CH, et al. Hippocampal mossy cell involvement in behavioral and neurogenic responses to chronic antidepressant treatment. Mol Psychiatry. 2020;25:1215–28. https://doi.org/10.1038/s41380-019-0384-6
27. Hill AS, Sahay A, Hen R. Increasing adult hippocampal neurogenesis is sufficient to reduce anxiety and depression-like behaviors. Neuropsychopharmacol. 2015;40:2368–78. https://doi.org/10.1038/npp.2015.85
28. Malberg JE, Eisch AJ, Nestler EJ, Duman RS. Chronic antidepressant treatment increases neurogenesis in adult rat hippocampus. J Neurosci. 2000;20:9104–10.
29. Samuels BA, Anacker C, Hu A, Levinstein MR, Pickenhagen A, Tsetsenis T, et al. 5-HT1A receptors on mature dentate gyrus granule cells are critical for the antidepressant response. Nat Neurosci. 2015;18:1606–16. https://doi.org/10.1038/nn.4116
30. Samuels BA, Hen R. Neurogenesis and affective disorders. Eur J Neurosci. 2011;33:1152–9. https://doi.org/10.1111/j.1460-9568.2011.07614.x
31. Amaral DG, Scharfman HE, Lavenex P. The dentate gyrus: fundamental neuroanatomical organization (dentate gyrus for dummies). Prog braRes. 2007;163:3–22. https://doi.org/10.1016/S0079-6123(07)63001-5

32. Scharfman HE. The enigmatic mossy cell of the dentate gyrus. Nat Rev Neurosci. 2016;17:562–75. https://doi.org/10.1038/nrn.2016.87
33. Yohn CN, Dieterich A, Maita I, Bazer AS, Diethorn E, Ma D, et al. Behavioral response to fluoxetine in both female and male mice is modulated by dentate gyrus granule cell activity. Neurobiol Stress. 2020;13:100257. https://doi.org/10.1016/j.ynstr.2020.100257
34. Kobayashi K, Ikeda Y, Sakai A, Yamasaki N, Haneda E, Miyakawa T, et al. Reversal of hippocampal neuronal maturation by serotonergic antidepressants. Proc Natl Acad Sci USA. 2010;107:8434–9. https://doi.org/10.1073/pnas.0912690107
35. Heiman M, Kulicke R, Fenster RJ, Greengard P, Heintz N. Cell type–specific mRNA purification by translating ribosome affinity purification (TRAP). Nat Protoc. 2014;9:1282–91. https://doi.org/10.1038/nprot.2014.085
36. Pittenger C, Duman RS. Stress, depression, and neuroplasticity: a convergence of mechanisms. Neuropsychopharmacol. 2008;33:88–109. https://doi.org/10.1038/sj.npp.1301574
37. Christiansen SH, Olesen MV, Wörtwein G, Woldbye DPD. Fluoxetine reverts chronic restraint stress-induced depression-like behaviour and increases neuropeptide Y and galanin expression in mice. Behavioural Brain Res. 2011;216:585–91. https://doi.org/10.1016/j.bbr.2010.08.044
38. Biever A, Valjent E, Puighermanal E. Ribosomal Protein S6 Phosphorylation in the Nervous System: From Regulation to Function. Front Mol Neurosci. 2015;8:75. https://doi.org/10.3389/fnmol.2015.00075
39. Mahoney SJ, Dempsey JM, Blenis J. Cell signaling in protein synthesis ribosome biogenesis and translation initiation and elongation. Prog Mol Biol Transl Sci. 2009;90:53–107. https://doi.org/10.1016/S1877-1173(09)90002-3
40. Knight ZA, Tan K, Birsoy K, Schmidt S, Garrison JL, Wysocki RW, et al. Molecular profiling of activated neurons by phosphorylated ribosome capture. Cell. 2012;151:1126–37. https://doi.org/10.1016/j.cell.2012.10.039
41. Meyuhas O. Ribosomal Protein S6 Phosphorylation: Four Decades of Research. Int Rev Cell Mol Biol. 2015;320:41–73. https://doi.org/10.1016/bs.ircmb.2015.07.006
42. Mundrucz L, Kecskés A, Henn-Mike N, Kóbor P, Buzás P, Vennekens R, et al. TRPM4 regulates hilar mossy cell loss in temporal lobe epilepsy. BMC Biol. 2023;21:96. https://doi.org/10.1186/s12915-023-01604-3
43. Hochgerner H, Zeisel A, Löbnnerberg P, Linnarsson S. Conserved properties of dentate gyrus neurogenesis across postnatal development revealed by single-cell RNA sequencing. Nat Neurosci. 2018;21:290–9. https://doi.org/10.1038/s41593-017-0056-2
44. Fujise N, Liu Y, Hori N, Kosaka T. Distribution of calretinin immunoreactivity in the mouse dentate gyrus: II. Mossy cells, with special reference to their dorsoventral difference in calretinin immunoreactivity. Neurosci. 1998;82:181–200.
45. Celio MR. Calbindin D-28k and parvalbumin in the rat nervous system. Neuroscience. 1990;35:375–475. https://doi.org/10.1016/0306-4522(90)90091-h
46. Etter G, Krezel W. Dopamine D2 receptor controls hilar mossy cells excitability. Hippocampus. 2014;24:725–32. https://doi.org/10.1002/hipo.22280
47. Fujise N, Liu Y, Hori N, Kosaka T. Distribution of calretinin immunoreactivity in the mouse dentate gyrus: II. Mossy cells, with special reference to their dorsoventral difference in calretinin immunoreactivity. Neuroscience. 1998;82:181–200. https://doi.org/10.1016/s0306-4522(97)00261-3
48. Li G, Berger O, Han SM, Paredes M, Wu NC, Pleasure SJ. Hilar mossy cells share developmental influences with dentate granule neurons. Dev Neurosci. 2008;30:255–61. https://doi.org/10.1159/000110347
49. Gangarossa G, Longueville S, De Bundel D, Perroy J, Hervé D, Girault JA, et al. Characterization of dopamine D1 and D2 receptor-expressing neurons in the mouse hippocampus. Hippocampus. 2012;22:2199–207. https://doi.org/10.1002/hipo.22044
50. Yohn CN, Gergues MM, Samuels BA. The role of 5-HT receptors in depression. Mol Brain. 2017;10:28. https://doi.org/10.1186/s13041-017-0306-y
51. Johnson GC, Parsons R, May V, Hammack SE. The role of pituitary adenylate cyclase-activating polypeptide (PACAP) signaling in the hippocampal dentate gyrus. Front Cell Neurosci. 2020;14:111. https://doi.org/10.3389/fncel.2020.00111
52. Hashimoto R, Hashimoto H, Shintani N, Ohi K, Hori H, Saitoh O, et al. Possible association between the pituitary adenylate cyclase-activating polypeptide (PACAP) gene and major depressive disorder. Neurosci Lett. 2010;468:300–2. https://doi.org/10.1016/j.neulet.2009.11.019
53. Hammack SE, May V. Pituitary adenylate cyclase activating polypeptide in stress-related disorders: data convergence from animal and human studies. Biol psychiatry. 2015;78:167–77. https://doi.org/10.1016/j.biopsych.2014.12.003
54. Ressler KJ, Mercer KB, Bradley B, Jovanovic T, Mahan A, Kerley K, et al. Post-traumatic stress disorder is associated with PACAP and the PAC1 receptor. Nature. 2011;470:492–7. https://doi.org/10.1038/nature09856
55. Ross RA, Hoeppner SS, Hellberg SN, O'Day EB, Rosencrans PL, Ressler KJ, et al. Circulating PACAP peptide and PAC1R genotype as possible transdiagnostic biomarkers for anxiety disorders in women: a preliminary study. Neuropsychopharmacol. 2020;45:1125–33. https://doi.org/10.1038/s41386-020-0604-4
56. Van Doorn CE, Zelows MM, Jaramillo AA. Pituitary adenylate cyclase-activating polypeptide plays a role in neuropsychiatric and substance use disorders: sex-specific perspective. Front Neurosci. 2025;19:1545810. https://doi.org/10.3389/fnins.2025.1545810
57. Steru L, Chermat R, Thierry B, Simon P. The tail suspension test: a new method for screening antidepressants in mice. Psychopharmacology. 1985;85:367–70. https://doi.org/10.1007/bf00428203
58. Surget A, Saxe M, Leman S, Ibarguen-Vargas Y, Chalon S, Griebel G, et al. Drug-dependent requirement of hippocampal neurogenesis in a model of depression and of antidepressant reversal. Biol psychiatry. 2008;64:293–301. https://doi.org/10.1016/j.biopsych.2008.02.022
59. Santarelli L, Saxe M, Gross C, Surget A, Battaglia F, Dulawa S, et al. Requirement of hippocampal neurogenesis for the behavioral effects of antidepressants. Science. 2003;301:805–9. https://doi.org/10.1126/science.1083328
60. Dagestad G, Kuipers SD, Messaoudi E, Bramham CR. Chronic fluoxetine induces region-specific changes in translation factor eIF4E and eEF2 activity in the rat brain. Eur J Neurosci. 2006;23:2814–8. https://doi.org/10.1111/j.1460-9568.2006.04817.x
61. Li N, Lee B, Liu RJ, Banasr M, Dwyer JM, Iwata M, et al. mTOR-dependent synapse formation underlies the rapid antidepressant effects of NMDA antagonists. Science. 2010;329:959–64. https://doi.org/10.1126/science.1190287
62. Li N, Liu RJ, Dwyer JM, Banasr M, Lee B, Son H, et al. Glutamate N-methyl-D-aspartate receptor antagonists rapidly reverse behavioral and synaptic deficits caused by chronic stress exposure. Biol psychiatry. 2011;69:754–61. https://doi.org/10.1016/j.biopsych.2010.12.015
63. Xu D, Wang C, Zhu X, Zhao W, Jiang B, Cui S, et al. The antidepressant-like effects of fluvoxamine in mice involve the mTOR signaling in the hippocampus and prefrontal cortex. Psychiat Res. 2020;285:112708. https://doi.org/10.1016/j.psychres.2019.112708
64. Karayol R, Medrihan L, Warner-Schmidt JL, Fait BW, Rao MN, Holzner EB, et al. Serotonin receptor 4 in the hippocampus modulates mood and anxiety. Mol Psychiatry. 2021;26:2334–49. https://doi.org/10.1038/s41380-020-00994-y
65. van den Pol AN. Neuropeptide transmission in brain circuits. Neuron. 2012;76:98–115. https://doi.org/10.1016/j.neuron.2012.09.014
66. Gołyszny M, Obuchowicz E. Are neuropeptides relevant for the mechanism of action of SSRIs? Neuropeptides. 2019;75:1–17. https://doi.org/10.1016/j.npep.2019.02.002
67. Shen M, Lv D, Liu X, Li S, Chen Y, Zhang Y, et al. Essential roles of neuropeptide VGF regulated TrkB/mTOR/BICC1 signaling and phosphorylation of AMPA receptor subunit GluA1 in the rapid antidepressant-like actions of ketamine in mice. Brain Res Bull. 2018;143:58–65. https://doi.org/10.1016/j.brainresbull.2018.10.004
68. Zhang HL, Sun Y, Wu ZJ, Yin Y, Liu RY, Zhang JC, et al. Hippocampal PACAP signaling activation triggers a rapid antidepressant response. Mil Med Res. 2024;11:49 https://doi.org/10.1186/s40779-024-00548-1
69. Lu X, Barr AM, Kinney JW, Sanna P, Conti B, Behrens MM, et al. A role for galanin in antidepressant actions with a focus on the dorsal raphe nucleus. Proc Natl Acad Sci. 2005;102:874–9. https://doi.org/10.1073/pnas.0408891102
70. Medrihan L, Sagi Y, Inde Z, Krupa O, Daniels C, Peyrache A, et al. Initiation of Behavioral Response to Antidepressants by Cholecystokinin Neurons of the Dentate Gyrus. Neuron. 2017;95:564–76.e564. https://doi.org/10.1016/j.neuron.2017.06.044
71. Asim M, Wang H, Waris A, He J. Basolateral amygdala parvalbumin and cholecystokinin-expressing GABAergic neurons modulate depressive and anxiety-like behaviors. Transl Psychiat. 2024;14:418 https://doi.org/10.1038/s41398-024-03135-z
72. Zhang X, Asim M, Fang W, Md Monir H, Wang H, Kim K, et al. Cholecystokinin B receptor antagonists for the treatment of depression via blocking long-term potentiation in the basolateral amygdala. Mol Psychiatry. 2023;28:3459–74. https://doi.org/10.1038/s41380-023-02127-7
73. Kim YK, Kim OY, Song J. Alleviation of Depression by Glucagon-Like Peptide 1 Through the Regulation of Neuroinflammation, Neurotransmitters, Neurogenesis, and Synaptic Function. Front Pharmacol. 2020;11:1270. https://doi.org/10.3389/fphar.2020.01270
74. Wei J, Zheng H, Li G, Chen Z, Fang G, Yan J. Involvement of oxytocin receptor deficiency in psychiatric disorders and behavioral abnormalities. Front Cell Neurosci. 2023;17:1164796. https://doi.org/10.3389/fncel.2023.1164796
75. Filliol D, Ghozland S, Chluba J, Martin M, Matthes HW, Simonin F, et al. Mice deficient for δ- and μ-opioid receptors exhibit opposing alterations of emotional responses. Nat Genet. 2000;25:195–200. https://doi.org/10.1038/76061
76. Yoshitake T, Wang FH, Kuteeva E, Holmberg K, Yamaguchi M, Crawley JN, et al. Enhanced hippocampal noradrenaline and serotonin release in galanin-overexpressing mice after repeated forced swimming test. Proc Natl Acad Sci. 2004;101:354–9. https://doi.org/10.1073/pnas.0307042101

77. Arimura A, Shioda S. Pituitary adenylate cyclase activating polypeptide (PACAP) and its receptors: neuroendocrine and endocrine interaction. Front Neuroendocrinol. 1995;16:53–88. https://doi.org/10.1006/frne.1995.1003
78. Vaudry D, Gonzalez BJ, Basille M, Yon L, Fournier A, Vaudry H. Pituitary Adenylate Cyclase-Activating Polypeptide and Its Receptors: From Structure to Functions. Pharmacol Rev. 2000;52:269–324.
79. Starr ER, Margiotta JF. Pituitary adenylate cyclase activating polypeptide induces long-term, transcription-dependent plasticity and remodeling at autonomic synapses. Mol Cell Neurosci. 2017;85:170–82. https://doi.org/10.1016/j.mcn.2017.10.002
80. Boucher MN, May V, Braas KM, Hammack SE. PACAP orchestration of stress-related responses in neural circuits. Peptides. 2021;142:170554. https://doi.org/10.1016/j.peptides.2021.170554
81. Singh A, Shim P, Naeem S, Rahman S, Lutfy K. Pituitary adenylyl cyclase-activating polypeptide modulates the stress response: the involvement of different brain areas and microglia. Front Psychiatry. 2024;15:1495598. https://doi.org/10.3389/fpsyt.2024.1495598
82. Ebner K, Fontebasso V, Ferro F, Singewald N, Hannibal J. PACAP regulates neuroendocrine and behavioral stress responses via CRF-containing neurons of the rat hypothalamic paraventricular nucleus. Neuropsychopharmacol. 2025;50:519–30. https://doi.org/10.1038/s41386-024-02016-9
83. Velasco ER, Florido A, Flores Á, Senabre E, Gomez-Gomez A, Torres A, et al. PACAP-PAC1R modulates fear extinction via the ventromedial hypothalamus. Nat Commun. 2022;13:4374 https://doi.org/10.1038/s41467-022-31442-w
84. Otto C, Martin M, Wolfer DP, Lipp HP, Maldonado R, Schütz G. Altered emotional behavior in PACAP-type-I-receptor-deficient mice. Brain Res Mol Brain Res. 2001;92:78–84. https://doi.org/10.1016/s0169-328x(01)00153-x
85. Hashimoto H, Hashimoto R, Shintani N, Tanaka K, Yamamoto A, Hatanaka M, et al. Depression-like behavior in the forced swimming test in PACAP-deficient mice: amelioration by the atypical antipsychotic risperidone. J neurochemistry. 2009;110:595–602. https://doi.org/10.1111/j.1471-4159.2009.06168.x
86. Reichenstein M, Rehavi M, Pinhasov A. Involvement of pituitary adenylate cyclase activating polypeptide (PACAP) and its receptors in the mechanism of antidepressant action. J Mol Neurosci. 2008;36:330–8. https://doi.org/10.1007/s12031-008-9116-0
87. Marcus SM, Young EA, Kerber KB, Kornstein S, Farabaugh AH, Mitchell J, et al. Gender differences in depression: Findings from the STAR*D study. J Affect Disord. 2005;87:141–50. https://doi.org/10.1016/j.jad.2004.09.008
88. Weissman MM, Bland RC, Canino GJ, Greenwald S, Hwu HG, Joyce PR, et al. Prevalence of suicide ideation and suicide attempts in nine countries. Psychol Med. 1999;29:9–17. https://doi.org/10.1017/S0033291798007867
89. Wilker S, Kolassa S, Ibrahim H, Rajan V, Pfeiffer A, Catani C, et al. Sex differences in PTSD risk: evidence from post-conflict populations challenges the general assumption of increased vulnerability in females. Eur J Psychotraumatol. 2021;12:1930702. https://doi.org/10.1080/20008198.2021.1930702
90. Mercer KB, Dias B, Shafer D, Maddox SA, Mulle JG, Hu P, et al. Functional evaluation of a PTSD-associated genetic variant: estradiol regulation and ADCYAP1R1. Transl Psychiat. 2016;6:e978. https://doi.org/10.1038/tp.2016.241
91. Snyder JS, Soumier A, Brewer M, Pickel J, Cameron HA. Adult hippocampal neurogenesis buffers stress responses and depressive behaviour. Nature. 2011;476:458–61. https://doi.org/10.1038/nature10287
92. Botterill JJ, Vinod KY, Gerencer KJ, Teixeira CM, LaFrancois JJ, Scharfman HE. Bidirectional regulation of cognitive and anxiety-like behaviors by dentate gyrus mossy cells in male and female mice. J Neurosci. 2021;41:2475–95. https://doi.org/10.1523/JNEUROSCI.1724-20.2021

ACKNOWLEDGEMENTS

This research was supported by the Basic Science Research Program through the National Research Foundation of Korea (NRF), funded by the Ministry of Education (2020R1I1A1A0107023611 to SJO, RS-2023-00237235 to SJO); the NRF funded by the Korea government (MSIT) (2021R1A2C1009454 to YSO); the NRF funded by the Korea government (MSIT) (RS-2024-00415347); the Basic Science Research Program through NRF funded by the Ministry of Education (2020R1A6A1A03040516); the NRF funded by the MSIT (RS-2021-NR057183); the DGIST R&D Program of the Ministry of Science and ICT (24-KUJoint-05); the National Institute on Aging (NIA), National Institute of Health (NIH) (1RF1AG047779 to JP).

AUTHOR CONTRIBUTIONS

S.J.O., J.J and Y.S.O. designed the experiments. S.J.O. performed and analyzed the behavior test. J.J., J.R. and J.H.Y performed, analyzed, and interpreted translatomic experiments. S.J.O., M.J, G.J., Y.S.J. and C.H.S. performed and analyzed Western blot and immunofluorescence data. S.J.O., J.R, K.L., H.C. and Y.S.O. discussed the data and corrections to the manuscript. S.J.O., Y.S.O. wrote the paper. All the authors approved the final version of the manuscript. We gratefully acknowledge Dr. Paul Greengard at The Rockefeller University for his generous support, and Assia Mouri for her technical assistance with GC-TRAP.

FUNDING

Open Access funding enabled and organized by DGIST (Daegu Gyeongbuk Institute of Science & Technology).

COMPETING INTERESTS

The authors declare no competing interests.

ETHICS APPROVAL

All animal experiments were conducted in accordance with the NIH Guide for the Care and Use of Laboratory Animals and complied with relevant national and institutional guidelines. Experimental protocols were approved by the Animal Care and Use Committee of the Daegu Gyeongbuk Institute of Science & Technology (IACUC #20011503-03) and the Rockefeller University (IACUC #14686-H).

ADDITIONAL INFORMATION

Supplementary information The online version contains supplementary material available at https://doi.org/10.1038/s41380-026-03461-2.

Correspondence and requests for materials should be addressed to Yong-Seok Oh.

Reprints and permission information is available at http://www.nature.com/reprints

Publisher's note Springer Nature remains neutral with regard to jurisdictional claims in published maps and institutional affiliations.